

**E.I. Rogacheva<sup>1</sup>, A.V. Budnik<sup>1</sup>, A.G. Fedorov<sup>2</sup>, A.S. Krivonogov<sup>3</sup>, P.V. Mateychenko<sup>3</sup>**

<sup>1</sup>National Technical University “Kharkiv Polytechnic Institute”,  
21 Frunze St., Kharkiv 61002, Ukraine

<sup>2</sup>Institute for Scintillation Materials NAS of Ukraine, 60 Lenin Ave., Kharkiv, 61001, Ukraine

<sup>3</sup>Institute for Single Crystals NAS of Ukraine, 60 Lenin Ave., Kharkiv, 61001, Ukraine

---

**STRUCTURE OF  $p$ - $Bi_2Te_3$  THIN FILMS PREPARED BY SINGLE SOURCE  
THERMAL EVAPORATION IN VACUUM**

---

*The growth mechanism, microstructure, and crystal structure of thin  $Bi_2Te_3$  films with thicknesses  $d = 28 - 620$  nm prepared by thermal evaporation of stoichiometric  $Bi_2Te_3$  crystals in vacuum onto glass substrates were studied using X-ray diffraction, scanning electron microscopy, energy dispersive spectroscopy, and atomic force microscopy. The obtained thin films were polycrystalline, exhibited  $p$ -type conductivity and did not contain any other phases except for  $Bi_2Te_3$ . It was shown that with increasing film thickness, the crystallite size increased up to  $\sim 700$ - $800$  nm. It was established that the preferential orientation of crystallite growth was  $[00l]$  direction corresponding to a trigonal axis  $C_3$  in hexagonal lattice. When the film thickness exceeded  $\sim 200$ - $250$  nm, along with reflections from  $(00l)$  planes, reflections from other planes appeared, which indicated a certain disorientation of crystallites. The results obtained show that using a simple and inexpensive method of thermal evaporation from a single source and choosing optimal technological parameters, one can grow thin  $p$ - $Bi_2Te_3$  films of sufficiently high quality.*

**Key words:** bismuth telluride, thermal evaporation, thin film, thickness, structure, growth orientation.

## **Introduction**

$Bi_2Te_3$  semiconductor compound and  $Bi_2Te_3$ -based solid solutions belong to the best low-temperature thermoelectric (TE) materials, which are widely used in the manufacture of different types of refrigerating devices [1-4]. A growing interest in low-dimensional nanostructures based on bismuth telluride [5-7] stimulates conducting detailed studies of properties of the indicated materials in the thin film state and establishing correlations among technological parameters, structure, and TE characteristics. In recent years, the interest in studying bulk crystals and thin films of  $Bi_2Te_3$  has grown even more after the discovery of new unique physical objects – topological insulators. It was established that  $Bi_2Te_3$  possesses properties of a 3D topological insulator, which attracted attention to studies of thin  $Bi_2Te_3$  films, in which the contribution of the surface layer to electrical conductivity increases in comparison with bulk crystals, thus making it possible to reveal the specificity of topological objects [8-10]. Works have appeared which showed a connection between topological and TE properties and pointed out the possibility to use this fact in searching for principally new ways of increasing TE efficiency [11-19].

$Bi_2Te_3$  crystallizes in a rhombohedral structure (space group  $R3m-D_{3d}^5$ ) [2, 4]. Often for describing  $Bi_2Te_3$  structure, instead of rhombohedral a hexagonal unit cell is used whose parameters correspond to  $a = 0.4386$  nm and  $c = 3.0497$  nm [2, 4]. The structure is composed of five-layer packets

(quintets) –  $\text{Te}^1$ –  $\text{Bi}$ –  $\text{Te}^2$ –  $\text{Bi}$ –  $\text{Te}^1$  (indices 1 and 2 denote different positions of  $\text{Te}$  atoms in the crystal lattice), perpendicular to a third-order symmetry axis (a trigonal axis  $C_3$  in a hexagonal lattice). Within each layer, similar atoms constitute a hexagonal flat lattice forming a hexagonal close packing with atoms of lower layers. Chemical bonds within quintets are predominantly covalent-ionic, whereas between quintets there are weak van der Waals bonds. This determines a low mechanical strength, easy splitting of crystals along cleavage planes (perpendicular to a  $C_3$  axis) and substantial anisotropy of all physical properties of  $\text{Bi}_2\text{Te}_3$  single crystals.

$\text{Bi}_2\text{Te}_3$  has a narrow homogeneity region (59.75 – 60.2 at.%  $\text{Te}$  at 770 K [20]) in the  $\text{Bi} - \text{Te}$  system. The stoichiometric  $\text{Bi}_2\text{Te}_3$  (60.0 at.%  $\text{Te}$ ) exhibits  $p$ -type conductivity due to the presence of anti-site defects  $\text{BiTe}$ .

$\text{Bi}_2\text{Te}_3$  films can be grown by a variety of methods: thermal evaporation in vacuum from a single source [21-30], thermal co-evaporation from two sources [31-33], hot wall epitaxy [34-36], quasi-closed volume technique [37], ion-beam deposition [38], magnetron sputtering [26, 39], molecular-beam epitaxy [27-29, 40], liquid phase epitaxy [30], metal organic chemical vapor deposition [41], laser deposition [42-44], explosive evaporation [45] and so on. Both amorphous and crystalline materials can be used as substrates. It was established that on amorphous substrates (glass [21-26, 39],  $\text{SiO}_2$  [34-36], kapton [35, 31]), films grow in an island-like fashion, while on crystalline substrates ( $\text{BaF}_2$  [27],  $\text{Si}$  [34, 28, 36, 40], sapphire [29]) both island-like [27] and layer-by-layer [27-29] growth can be realized. The growth mechanism, film morphology, grain size, and grain crystallographic orientation depend on the film preparation technique and technological parameters.

For anisotropic materials like  $\text{Bi}_2\text{Te}_3$ , the transport properties depend significantly on the direction in the crystal. For example, it was reported in [39] that in  $\text{Bi}_2\text{Te}_3$  films the preferential growth of (00 $l$ ) planes leads to substantially higher values of electrical conductivity, charge carrier mobility and the Seebeck coefficient in comparison with the preferential growth of (015) planes. That is why, when growing films, it is important to know and to control the preferential growth direction.

The growth mechanism and structure of  $\text{Bi}_2\text{Te}_3$  thin films prepared by thermal evaporation in vacuum from a single source onto glass substrates were investigated in few works [23-25]. In [23], where the authors did not indicate the substrate temperature, it was established using X-ray diffraction analysis that in films with thicknesses  $d = 36 - 330$  nm deposited onto glass substrates the preferential orientation of crystallites corresponded to [015] direction, although under increasing film thickness additional peaks appeared in X-ray diffraction patterns, which indicated a partial grain disorientation. In [24], X-ray diffraction analysis was used to study the structure of  $\text{Bi}_2\text{Te}_3$  films of the fixed thickness ( $d = 100$  nm) but deposited onto glass substrates heated to different temperatures ( $T_S = 303 - 573$  K). The authors found out that for all values of  $T_S$  the preferential growth takes place along the [015] direction, although there is some disorientation of grains relative to this direction. Note that in [23, 24] the films were not subjected to annealing which could improve the quality of their structure, and perhaps because of this the crystallite size  $D$  in the films was small ( $D = 15 - 45$  nm). The authors of [25] investigated sufficiently thick  $\text{Bi}_2\text{Te}_3$  films ( $d = 170 - 342$  nm), which were annealed at  $T = 443$  K for one hour. They reported that the film with thickness  $d = 342$  nm had the preferential orientation of growth along the [015] direction, which manifests clearly only after annealing. With increasing film thickness from 170 nm to 342 nm, the grain size increased from 60 up to 160 nm. Thus, in the available works on  $\text{Bi}_2\text{Te}_3$  films prepared by thermal evaporation of  $\text{Bi}_2\text{Te}_3$  crystals in vacuum onto glass substrates and characterized by X-ray diffraction method, authors reported their observation of preferential orientation only along the [015] axis. There arises a question whether it is possible to

obtain another preferential orientation, specifically [00 $l$ ], which as was mentioned above is more desirable because of the possibility to obtain higher values of TE figure of merit.

The goal of the present work is to carry out a detailed comprehensive investigation of the microstructure and crystal structure of thin Bi<sub>2</sub>Te<sub>3</sub> films grown by thermal evaporation of stoichiometric bismuth telluride crystals in vacuum and subsequent condensation onto glass substrates.

## **Experimental procedure**

As a charge for thin films preparation, *p*-type Bi<sub>2</sub>Te<sub>3</sub> polycrystal of stoichiometric composition was used. Crystal synthesis was made by direct alloying of Bi and Te of high purity (99.999 at. %) in evacuated quartz ampoules at a temperature of (1020 ± 10) K for 5 – 6 hours with subsequent annealing at 670 K for 300 hours.

Films of thickness  $d = 28\text{--}620$  nm were grown by method of thermal evaporation in vacuum ( $\sim 10^{-5}$  Pa) of Bi<sub>2</sub>Te<sub>3</sub> polycrystal of stoichiometric composition and subsequent condensation onto glass substrates heated to temperature  $T_s = 500$  K. Condensation rate was 0.1 – 0.3 nm/s. Prior to deposition, substrates were consecutively cleaned with hydrochloric acid, distilled water and 95% alcohol. Immediately after deposition, grown films in the same vacuum chamber were annealed at a temperature of  $T = 500$  K for 1 hour. For a simultaneous preparation of several films of different thickness  $d$  in one technological process, three substrate holders were installed at different distances from the source. Earlier we showed [21, 22] that the properties of Bi<sub>2</sub>Te<sub>3</sub> thin films are essentially dependent on the stoichiometry of source crystal, substrate temperature  $T_s$ , the presence or absence of annealing, annealing temperature, on which basis the above technological parameters were determined that corresponded to maximum values of TE power  $P = S^2\sigma$  ( $S$  is the Seebeck coefficient,  $\sigma$  is electric conductivity).

The thickness and roughness of films, as well as condensation rate, were controlled by quartz resonator. Calibration of resonator for film thicknesses less than  $d \sim 100$  nm was performed with the use of X-ray diffraction patterns of small-angle scattering by comparing the experimental and calculated diffraction patterns. At layer thicknesses  $d < 100$  nm close to primary beam an interference X-ray diffraction is observed, namely the Kissing oscillations whose period can be used to determine film thickness to an accuracy of 0.5 nm. Numerical simulation was performed with the use of Frenkel's formulae. For fitting of calculated curve to the experimental one two parameters were varied independently, namely film thickness and roughness. For large thicknesses ( $d > 100$  nm), quartz resonator was calibrated using MII-4 interferometer.

Chemical composition, homogeneity degree and films morphology were studied by electron probe analysis method with the use of scanning electron microscope (SEM) JSM-6390LV (Jeol Ltd., Japan), equipped with energy-dispersive X-ray spectrometer X-max N50. The surface morphology of films was also studied using atomic force microscope (AFM) Solver Pro NT-MDT. Crystal structure, phase composition and direction of preferential films growth were determined by X-ray structural analysis methods on DRON-2 diffractometer using Cu  $K_\alpha$  – radiation.

## **Experimental results**

Fig. 1, a shows X-ray diffraction pattern of Bi<sub>2</sub>Te<sub>3</sub> polycrystal which was used as a charge for preparation of thin films. All the lines on X-ray diffraction pattern corresponded to values given in ASTM standards for Bi<sub>2</sub>Te<sub>3</sub> (№ 15-863) [46], no additional phases were found.

Fig. 1, b-h show X-ray patterns of thin films of different thickness prepared with optimal technological parameters. The films have a marked crystalline structure, and all diffraction peaks correspond to Bi<sub>2</sub>Te<sub>3</sub> compound, no peaks of other phases were found. To demonstrate the influence of films preparation technology on their phase composition and structure, Fig. 2 shows X-ray patterns of films ( $d = 250$  nm) obtained at substrate temperature  $T_S = 320$  K without annealing (Fig. 2, a) and at substrate temperature  $T_S = 500$  K with annealing for one hour at 500 K (Fig. 2, b), i.e. prepared by the method used in the present paper. It can be seen that in the former case the film has a structure close to amorphous, with weakly expressed diffraction peaks, and the film has additional phases of Te and Bi<sub>3</sub>Te<sub>4</sub>. In this connection it can be assumed that due to higher partial pressure of Te vapour as compared to bismuth, during the initial stages of film deposition tellurium excess can be created on the substrate. As long as substrate temperature is sufficiently low ( $T_S = 320$  K), no intensive reevaporation of Te atoms occurs, and part of Te atoms precipitates into second phase. With further formation of the film, deficit of Te atoms can result in formation of Bi<sub>3</sub>Te<sub>4</sub> phase. High intensity of peak corresponding to (015) planes testifies to preferential formation in the film of hexagonal planes with respective structure.

As in seen in Fig. 1, b-e, in the films with thicknesses  $d$  lower than  $d \sim 140$  nm, the intensity of peaks (003), (006), (0 0 15), (0 0 18) and (0 0 21) is increased more than twice as compared to the bulk crystal with practically complete disappearance of peaks corresponding to other crystallographic planes. Essential increase of the intensity of peaks corresponding to these planes as compared to similar peaks of X-ray diffraction pattern of the source powder indicate the presence of texture in [001] direction. To confirm the presence of preferential orientation of crystallites along [00 $l$ ] direction, film of thickness  $d = 85$  nm (Fig. 1, h) was measured in a standard mode (in the initial position X-ray beam was oriented perpendicular to the film), and then the sample was rotated by 21.80°. As long as planes (0 0 21) and (0 1 20) are at an angle of 21.80° to each other, in the former case there is intensive peak only from (0 0 21) plane, and in the second case – only from (0 1 20) plane, confirming the presence of preferential orientation of all grains in one direction [0 0  $l$ ].

The authors [35, 36] attribute formation of texture in [0 0 1] direction to peculiarity of Bi<sub>2</sub>Te<sub>3</sub> growth on amorphous substrates which assure higher surface mobility of deposited substance atoms as compared to crystalline substance. This allows reaching sufficiently fast the state close to equilibrium, when the atoms of deposited substance occupy thermodynamically most advantageous positions on the substrate, which contributes to texture formation. Moreover, epitaxial growth peculiarities of layered structures with Van der Waals bonds [36, 37] and the absence of broken bonds on the substrate surface [34] cause the arrangement of layers with Van der Waals bonds along the film plane which in turn provides for orientation of crystallites in perpendicular direction [0 0 1] [37]. Strong anisotropy of growth rate assures a more intensive growth of crystallites along the directions perpendicular to texture direction, which contributes to fast intergrowth of crystallites in film plane, and growth rate of Bi<sub>2</sub>Te<sub>3</sub> films parallel to substrate surface proves to be a factor of 5 to 8 higher than growth rate perpendicular to it.

On the X-ray diffraction patterns of films with thicknesses more than  $d \sim 140$  nm (Fig. 1 f, g) along with reflexes (0 0  $l$ ) there appear peaks from crystallographic planes different from (0 0 1), the number increasing with increase in film thickness. This testifies to disorientation of crystallites and is likely to be a consequence of dislocation density growth and stress accumulation. Nevertheless, the intensity of peaks (0 0  $l$ ) for all films is almost not changed which testifies to the absence of essential disorientation in the direction of texture.

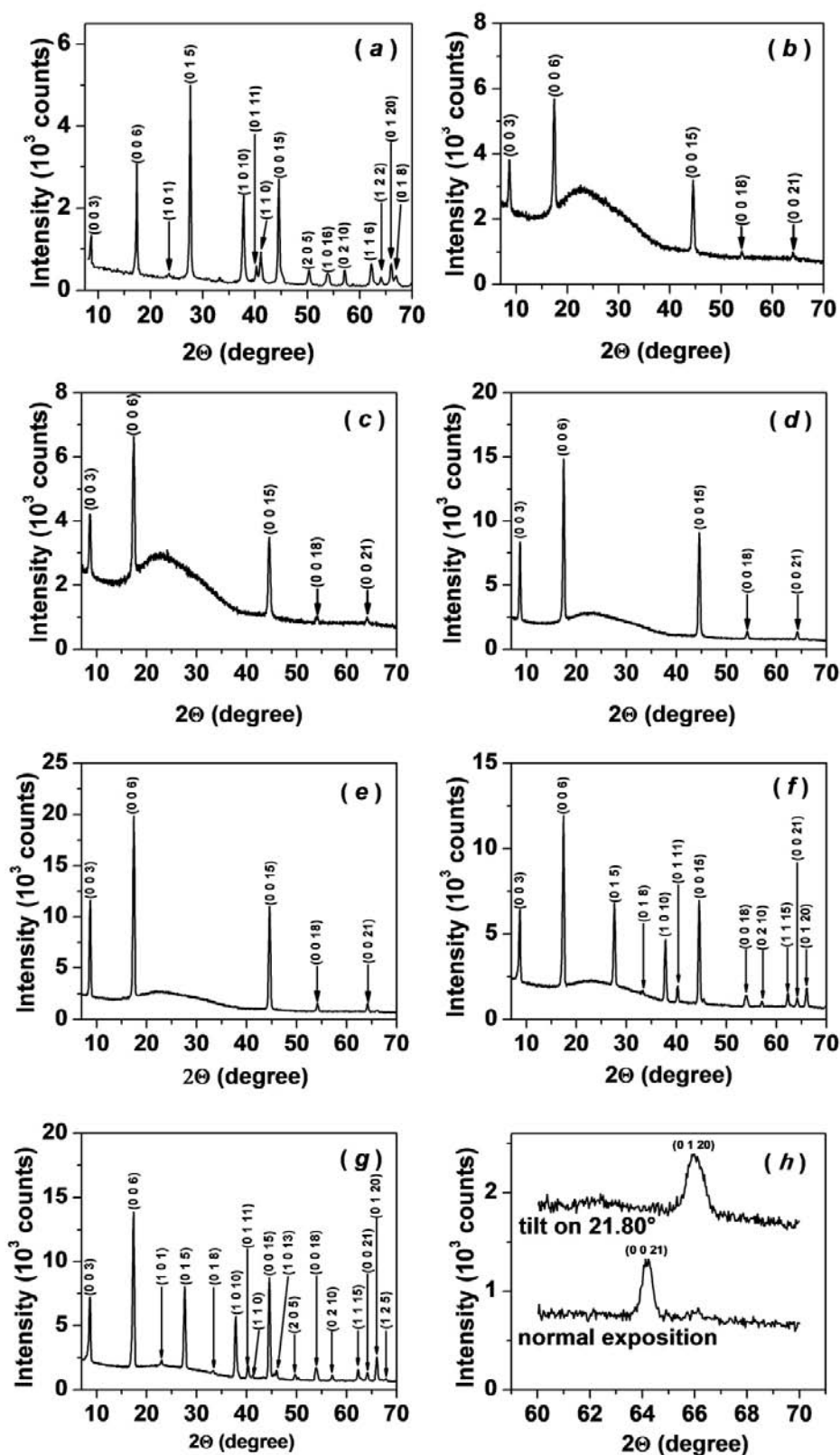


Fig. 1. X-ray diffraction patterns for polycrystalline  $\text{Bi}_2\text{Te}_3$  powder (a) and for thin films with different thicknesses:  $d = 38$  nm (b), 45 nm (c), 85 nm (d), 140 nm (e), 370 nm (f), 620 nm (g).  
 h: X-ray diffraction pattern for the thin film with  $d = 85$  nm is measured in a standard mode (with a X-ray beam oriented perpendicular to the film surface) and after rotating the sample by  $21.80^\circ$  (see the text).

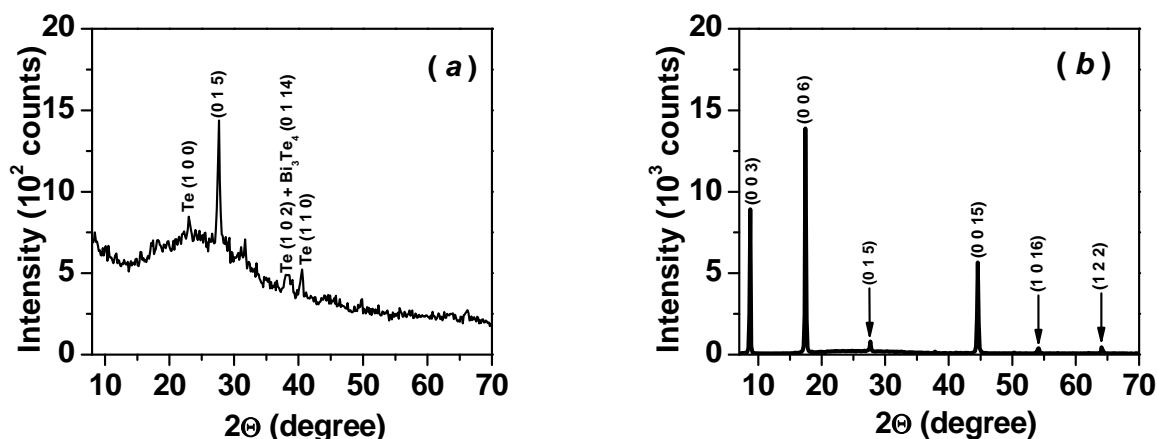


Fig. 2. X-ray diffraction patterns for  $\text{Bi}_2\text{Te}_3$  films with thicknesses  $d = 250$  nm prepared at the substrate temperature  $T_S = 320$  K without annealing (a) and at  $T_S = 500$  K with subsequent annealing at 500 K for one hour (b).

Studies of thin films by scanning electron microscopy method (Fig. 3) have confirmed that the films are polycrystalline and there are no second phase inclusions in them. The grains were of hexagonal shape (for illustrative purposes some grains are shown dashed) and their average size was increased with increase in film thickness (Fig. 4), which was in good agreement with the results of AFM. The results of energy-dispersive X-ray spectroscopy both at scanning along the sample surface and in the mode of probing from point to point have shown that all the films were characterized by high homogeneity degree and that within the error of this method one could speak of the conformity between the composition of the source polycrystal and that of grown films.

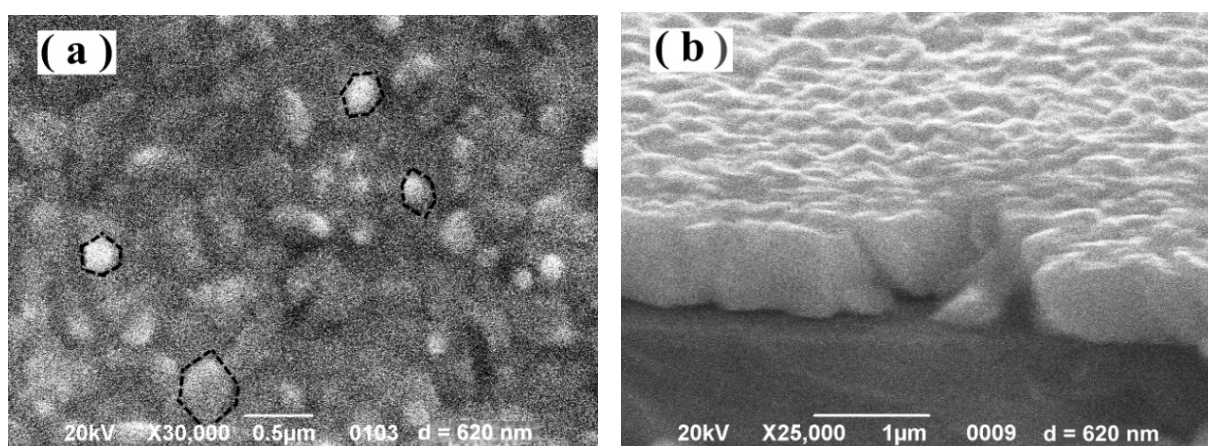


Fig. 3. Surface images obtained using a scanning electron microscope (SEM) for  $\text{Bi}_2\text{Te}_3$  film with thickness  $d = 620$  nm. a – no tilt, b - tilt angle  $70^\circ$ .

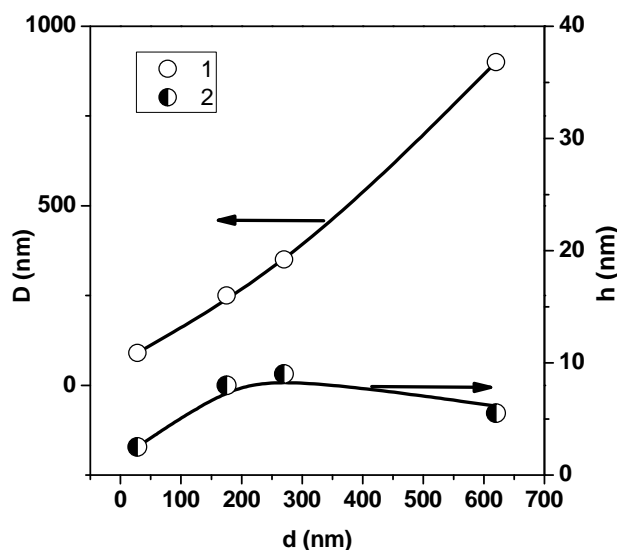


Fig. 4. Grain size  $D$  and roughness  $h$  as functions of  $p\text{-Bi}_2\text{Te}_3$  thin film thickness  $d$ .  
1 – grain size; 2 – roughness.

Fig. 5 represents the data of atomic force microscopy. On the obtained profilograms one can clearly see individual crystallites of mainly hexagonal shape, which points to their orientation in  $[0\ 0\ 1]$  direction perpendicular to film surface which is in good agreement with the results of X-ray structural analysis (Fig. 1), as well as with the data of scanning electron microscopy (Fig. 3). The sizes of crystallites  $D$  evaluated by two methods – SEM and AFM – practically coincide and show marked increase with increase in film thickness, reaching in the “thickest” of films under study ( $d = 620$  nm) the value of  $D \sim 850$  nm (Fig. 4). The roughness of films  $h$  with growth in their thickness  $d$  first increases (to  $d \sim 200 - 250$  nm), following which there is a tendency to  $h$  reduction (Fig. 4).

## Conclusions

A comprehensive study of growth mechanism, microstructure, and crystal structure of thin  $\text{Bi}_2\text{Te}_3$  films with thicknesses  $d = 28 - 620$  nm prepared by thermal evaporation of stoichiometric  $\text{Bi}_2\text{Te}_3$  crystals in vacuum onto glass substrates heated to  $T_s = 500$  K and subject to subsequent annealing at 500 K was performed using X-ray diffraction, scanning electron microscopy, energy dispersive spectroscopy, and atomic force microscopy.

It was established that both the initial crystal and all obtained thin films exhibited  $p$ -type conductivity and did not contain any other phases except for  $\text{Bi}_2\text{Te}_3$ .

It was shown that the obtained thin films were polycrystalline; with increasing film thickness, the grain size  $D$  of the films increased to  $D \sim 850$  nm, and roughness  $h$  increased with increasing film thickness to  $\sim d \sim 200\text{-}250$  nm, following which there was a tendency to reduction.

It was established that the preferential orientation of crystallite growth was  $[00l]$  direction corresponding to a trigonal axis  $C_3$  in hexagonal lattice. When the film thickness exceeded  $\sim 200\text{-}250$  nm, along with reflections from  $(00l)$  planes, reflections from other planes appeared, which indicated a certain disorientation of crystallites.

The results obtained show that using a simple and inexpensive method of thermal evaporation from a single source and choosing optimal technological parameters, one can grow thin  $p\text{-Bi}_2\text{Te}_3$  films of sufficiently high quality.

The work was performed with support from the State Foundation for Basic Research (Ukraine) (Grant #UU 42/006-2011) and US Civilian Research and Development Foundation (Grant # UKP-7074-KK-12).

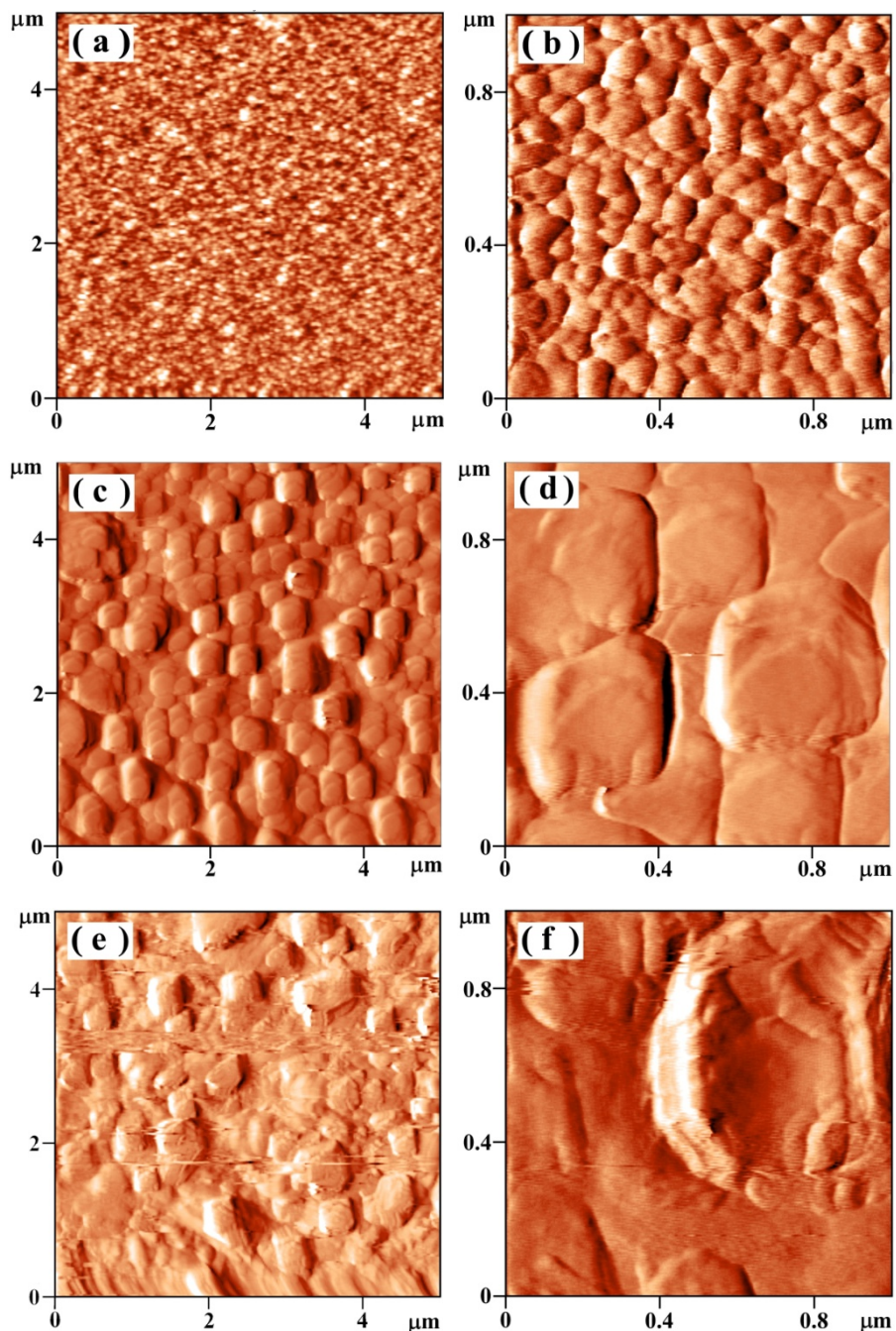


*Fig.5. AFM surface profilograms for Bi<sub>2</sub>Te<sub>3</sub> thin films with thickness  $d = 28$  nm:  $5 \times 5 \mu\text{m}$  (a),  $1 \times 1 \mu\text{m}$  (b);  $d = 175$  nm:  $5 \times 5 \mu\text{m}$  (c),  $1 \times 1 \mu\text{m}$  (d);  $d = 270$  nm:  $5 \times 5 \mu\text{m}$  (e),  $1 \times 1 \mu\text{m}$  (f).*



## References

1. L.I. Anatyshchuk, *Thermoelements and Thermoelectric Devices: Reference Book*, (Kyiv: Naukova Dumka, 1979).
2. H. Scherrer, S. Scherrer, Bismuth Telluride, Antimony Telluride and their Solid Solution (*CRC Handbook of thermoelectric Edited by D.M. Rowe, 1995*), P. 213–223.
3. L.E. Bell. Cooling, Heating, Generating Power, and Recovering Waste Heat with Thermoelectric Systems, *Science* **321**, 1457 (2008).
4. B.M.Goltsman, V.A.Kudinov, and I.A. Smirnov, *Semiconducting Thermoelectric Materials Based on Bi<sub>2</sub>Te<sub>3</sub>* (Moscow: Nauka, 1972) (in Russian).
5. L D. Hicks, M. S. Dresselhaus, Effect of Quantum-Well Structures on the Thermoelectric Figure of Merit, *Phys. Rev. B* **47**, 12727 (1993). DOI: <http://dx.doi.org/10.1103/PhysRevB.47.12727>
6. M.S. Dresselhaus, Yu-Ming Lin, T. Koga, S.B.Cronin, O. Rabin, M.R. Black, and G. Dresselhaus, In *Semiconductors and Semimetals: Recent Trends in Thermoelectric Materials Research III*, edited by T.M. Tritt, (Academic Press, San Diego, CA, 2001), pp. 1–121.
7. R. Venkatasubramanian, E. Siivola, T. Colpitts, and B. O’Quinn, Thin-Film Thermoelectric Devices with High Room-Temperature Figures of Merit, *Nature* **413**, 597 (2001). DOI: <http://dx.doi.org/10.1038/35098012>
8. L. Fu, C. L. Kane, Topological Insulators with Inversion Symmetry, *Phys Rev. B* **76**, 045302 (2007). DOI: <http://dx.doi.org/10.1103/PhysRevB.76.045302>
9. L. Muchler, F. Casper, B. Yan, S. Chadov, and C. Felser, Topological Insulators and Thermoelectric Materials, *Phys. Status Solidi RRL* **7**, 91 (2013). DOI: <http://dx.doi.org/10.1002/pssr.201206411>.
10. D. Culcer, Transport in Three-Dimensional Topological Insulators: Theory and Experiment, *Physica E* **44**(8), 860 (2012). DOI: <http://dx.doi.org/10.1016/j.physe.2011.11.003>.
11. D. Teweldebrhan, V. Goyal, M. Rahman, and A. Balandin, *Appl. Phys. Lett.* **96**, 053107 (2010).
12. Y. S. Hor, A. Richardella, P. Roushan, Y. Xia, J.G. Checkelsky, A. Yazdani, M. Z. Hasan, N.P. Ong, and R.J. Cava, *Phys. Rev. B* **79**, 195208 (2009).
13. Y.L. Chen, Z.K. Liu, J.G. Analytis, J.-H. Chu, H. J. Zhang, B. H. Yan, S.-K. Mo, R. G. Moore, and D. H. Lu, *Phys. Rev. Lett.* **105**, 266401 (2010).
14. P. Ghaemi, R.S.K. Mong, and J. Moore, *Phys. Rev. Lett.* **105**, 166603 (2010).
15. O.A. Tretiakov, Ar. Abanov, and Jairo Sinova, *Appl. Phys. Lett.* **99**, 113110 (2011).
16. Y. Sun, H. Cheng, S. Gao, Q. Liu, Z. Sun, C. Xiao, C. Wu, S. Wei, and Y. Xie, *J. Am. Chem. Soc.* **134**, 20294 (2012).
17. Z. Fan, J. Zheng, H.-Q. Wang, and J.-C. Zheng, *Nanoscale Research Letters* **7**, 570 (2012).
18. R. Takahashi and S. Murakami, *Semicond. Sci. Technol.* **27**, 124005 (2012).
19. L. MÜchler, F. Casper, B. Yan, S. Chadov, and C. Felser, *Phys. Stat. Solidi RRL* **7**, 91 (2013).
20. R.F. Brebrick, Homogeneity Ranges and Te<sub>2</sub>-Pressure along the Three-Phase Curves for Bi<sub>2</sub>Te<sub>3</sub>(c) and a 55–58 at.% Te, Peritectic Phase, *J. Phys. Chem. Sol.* **30**(3), 719, (1969). DOI: [http://dx.doi.org/10.1016/0022-3697\(69\)90026-2](http://dx.doi.org/10.1016/0022-3697(69)90026-2)
21. A. V. Budnik, E. I. Rogacheva, V. I. Pinegin, A. Yu. Sipatov, A. G. Fedorov, Effect of Initial Bulk Material Composition on Thermoelectric Properties of Bi<sub>2</sub>Te<sub>3</sub> Thin Films, *J. Electron. Mater.* **42** (7), 1324 (2013). DOI: <http://dx.doi.org/10.1007/s11664-012-2439-1>

22. A. V. Budnik, E. I. Rogacheva, A.Yu. Sipatov, Effect of Fabrication Technique on the Structure and Thermoelectric Properties of  $\text{Bi}_2\text{Te}_3$  films, *J. Thermoelectricity* **4**, 19 (2013).
23. R. Sathyamoorthy, J. Dheepa, Structural Characterization of Thermally Evaporated  $\text{Bi}_2\text{Te}_3$  Thin Films, *J. Phys.Chem. Solids* **68**(1), 111 (2007). DOI: <http://dx.doi.org/10.1016/j.jpics.2006.09.014>
24. B. Jariwala, D.V. Shah, V. Kheraj, Substrate Temperature Effect on Structural Properties of  $\text{Bi}_2\text{Te}_3$  Thin Films, *J. Nano- Electron. Phys.* **3**, 101 (2010).
25. F.S. Bahabri, Investigation of the Structural and Optical Properties of Bismuth Telluride ( $\text{Bi}_2\text{Te}_3$ ) Thin Films, *Life Science Journal* **9**(1), 290 (2012).
26. Y. Deng, H. Liang, Y. Wang, Z. Zhang, M. Tan, and J. Cui, Growth and Transport Properties of Oriented Bismuth Telluride Films, *J.Alloys and Compounds* **509**(18), 5683 (2011). DOI: <http://dx.doi.org/10.1016/j.jallcom.2011.02.123>
27. J.Numus, H. Bottner, H. Beyer, and A. Lambrecht, Epitaxial Bismuth Telluride Layers Grown on (111) Barium Fluoride Substrates Suitable for MQW-Growth, *18th International Conference on Thermoelectrics*, 696 (2000). DOI: <http://dx.doi.org/10.1109/ICT.1999.843481>
28. J. Krumrain, G. Mussler, S. Borisova, T. Stoica, L. Plucinski, C. M. Schneider, and D. Grützmacher, MBE Growth Optimization of Topological Insulator  $\text{Bi}_2\text{Te}_3$  Films, *J. Crystal Growth* **324** (1), 115 (2011). DOI: <http://dx.doi.org/10.1016/j.jcrysgro.2011.03.008>
29. J. J. Lee, F. T. Schmitt, R. G. Moore, I. M. Vishik, Y. Ma, and Z. X. Shen, Intrinsic Ultrathin Topological Insulators Grown via MBE Characterized by in-situ Angle Resolved Photoemission Spectroscopy, *Appl. Phys. Lett.* **101**, 013118 (2012). DOI: <http://dx.doi.org/>
30. C.Boulanger, Thermoelectric Material Electroplating: a Historical Review, *J. Electron. Mater.* **39**, 1818-1827 (2010). DOI: <http://dx.doi.org/10.1063/1.4733317>
31. L. M. Goncalve, C. Couto, P. Alpuim, A. G. Rolo, F. Völklein, and J. H. Correia, Optimization of Thermoelectric Properties on  $\text{Bi}_2\text{Te}_3$  Thin Films Deposited by Thermal Co-Evaporation, *Thin Solid Films* **518**(10), 2816 (2010). DOI: <http://dx.doi.org/10.1016/j.tsf.2009.08.038>
32. Luciana W. da Silva, Massoud Kaviany, and Ctirad Uher, Thermoelectric Performance of Films in the Bismuth–Tellurium and Antimony–Tellurium Systems, *J. Appl. Phys.* **97**(11), 1 (2005). DOI: <http://dx.doi.org/10.1063/1.1914948>
33. H. Zou, D.M. Rowe, and S.G.K.Williams, Peltier Effect in a Co-Evaporated  $\text{Sb}_2\text{Te}_3(\text{P})$ - $\text{Bi}_2\text{Te}_3(\text{N})$  Thin Film Thermocouple, *J. Appl. Phys.* **408**(1-2), 270 (2002). DOI: [http://dx.doi.org/10.1016/S0040-6090\(02\)00077-9](http://dx.doi.org/10.1016/S0040-6090(02)00077-9)
34. J. C. Tedenac, S. Dal Corso, A. Haidoux, S. Charar, and B. Liautard, Growth of Bismuth Telluride Thin Films by Hot Wall Epitaxy, Thermoelectric Properties, *Mat. Res. Soc. Symp. Proc.* 545, 93 (1998). DOI: <http://dx.doi.org/10.1557/PROC-545-93>
35. M. Ferhat, J. C. Tedenac, and J. Nagao, Mechanisms of Spiral Growth in  $\text{Bi}_2\text{Te}_3$  Thin Films Grown by the Hot–Wall–Epitaxy Technique, *Journal of Crystal Growth* **218**(2-4), 250 (2000). DOI: [http://dx.doi.org/10.1016/S0022-0248\(00\)00582-0](http://dx.doi.org/10.1016/S0022-0248(00)00582-0)
36. M. Ferhat, B. Liautard, G. Brun, J.C. Tedenac, M. Nouaoura, and L. Lassabatere, Comparative Studies between the Growth Characteristics of  $\text{Bi}_2\text{Te}_3$  Thin Films Deposited on  $\text{SiO}_2$ ,  $\text{Si}(100)$  and  $\text{Si}(111)$ , *J. Cryst. Growth* **167**(1-2), 122 (1996). DOI: [http://dx.doi.org/10.1016/0022-0248\(96\)00247-3](http://dx.doi.org/10.1016/0022-0248(96)00247-3)
37. O. Vigil–Galan, F. Cruz–Gandarilla, J. Fandino, F. Roy, J. Sastre–Hernandez, and G. Contreras–Puentes, Physical Properties of  $\text{Bi}_2\text{Te}_3$  and  $\text{Sb}_2\text{Te}_3$  Films Deposited by Close Space

- Vapor Transport, *Semicond. Sci. Technol.* **24**(2), 1 (2009). DOI: <http://dx.doi.org/10.1088/0268-1242/24/2/025025>
38. Z.-H. Zheng, P. Fan, G.-X. Lang, D.-P. Zhang, X.-M. Cai, and T.-B. Chen, Annealing Temperature Influence on Electrical Properties of Ion Beam Sputtered Bi<sub>2</sub>Te<sub>3</sub> Thin Films, *J. Phys. Chem. Solids.* **71** (12), 1713 (2010). DOI: <http://dx.doi.org/10.1016/j.jpcs.2010.09.012>
39. Y. Deng, Zh. Zhang, Y. Wang, Y. Xu, Preferential Growth of Bi<sub>2</sub>Te<sub>3</sub> Films with a Nanolayers Structure: Enhancement of Thermoelectric Properties Induced by Nanocrystal Boundaries, *J. Nanopart. Res.* **14**, 775 (2012). DOI: <http://dx.doi.org/10.1007/s11051-012-0775-y>
40. J. Krumrain, G. Mussler, S. Borisova, T. Stoica, L. Plucinski, C.M. Schneider, and D. Grutzmacher, MBE Growth Optimization of Topological Insulator Bi<sub>2</sub>Te<sub>3</sub> Films, *J. Crystal Growth* **324**(1), 115 (2011). DOI: <http://dx.doi.org/10.1016/j.jcrysgro.2011.03.008>
41. A. Giani, F. Pascal-Delannoy, A. Boyer, A. Foucaran, M. Gschwind, and P. Ancy, Elaboration of Bi<sub>2</sub>Te<sub>3</sub> by Metal Organic Chemical Vapor Deposition, *Thin Solid Films* **303**, (1-2), (1997) . DOI: [http://dx.doi.org/10.1016/S0040-6090\(97\)00089-8](http://dx.doi.org/10.1016/S0040-6090(97)00089-8)
42. A. Dauscher, A. Thomy, and H. Scherrer, Pulsed Laser Deposition of Bi<sub>2</sub>Te<sub>3</sub> Thin Films, *Thin Solid Films* **280**(1-2), 61 (1996). DOI: [http://dx.doi.org/10.1016/0040-6090\(95\)08221-2](http://dx.doi.org/10.1016/0040-6090(95)08221-2)
43. Li Bassi, A. Bailini, C. S. Casari, F. Donati, A. Mantegazza, M. Passoni, V. Russo, and C. E. Bottani, Thermoelectric Properties of Bi-Te Films with Controlled Structure and Morphology, *J. Appl. Phys.* **105**(12), 124307 (2009). DOI: <http://dx.doi.org/10.1063/1.3147870>.
44. R. S. Makala, K. Jagannadham, and B.C. Sales, Pulsed Laser Deposition of Bi<sub>2</sub>Te<sub>3</sub>-Based Thermoelectric Thin Films, *J. Appl Phys* **94** (6), 3907 (2003). DOI: <http://dx.doi.org/10.1063/1.1600524>
45. F. Volklein, V. Baier, U. Dillner, and E. Kessler, Transport Properties of Flash-Evaporated (Bi<sub>1-x</sub>Sb<sub>x</sub>)<sub>2</sub>Te<sub>3</sub> Films I: Optimization of Film Properties, *Thin Solid Films* **187** (2), 253 (1990). DOI: [http://dx.doi.org/10.1016/0040-6090\(90\)90047-H](http://dx.doi.org/10.1016/0040-6090(90)90047-H).
46. Powder Diffraction File, *Joint Committee on Powder Diffraction Standards* (Philadelphia, PA: ASTM, 1967).

Submitted 16.04.2015.